TUSKEGEE UNIVERSITY
SCHOOL OF ENGINEERING AND ARCHITECTURE
TUSKEGEE, ALABAMA

DEVELOPMENT OF CAPABILITY FOR CHARACTERIZATION OF CERAMIC/CERAMIC COMPOSITES PART - II

(High Temperature Characterization of SiCw/SiC Composites and Prediction of Flexural Properties by Energy Method)

Shaik Jeelani
Hassan Mahfuz
Anwarul Haque
Sirajus Salekeen

TECHNICAL REPORT

Prepared for

United States Airforce, Office of Scientific Research
Grant No. F-49620-89-C-0016DEF

SECURITY CLASSIFICATION OF THIS PAGE (When Data Entered)

REPORT DOCUMENTATION PAGE

READ INSTRUCTIONS BEFORE COMPLETING FORM

1. REPORT NUMBER: TU-AFSR- 2	2. GOVT ACCESSION NO.
3. RECIPIENT'S CATALOG NUMBER	
4. TITLE (and Subtitle): DEVELOPMENT OF CAPABILITY FOR CHARACTERIZATION OF CERAMIC/CERAMIC COMPOSITES-PART II (u)	5. TYPE OF REPORT & PERIOD COVERED: Technical - FINAL Dec.1., 1989-Nov.30, 1990
	6. PERFORMING ORG. REPORT NUMBER
7. AUTHOR(s): DR. SHANIK, JEELANI	8. CONTRACT OR GRANT NUMBER(s): AFOSR-TR- 92 0455 F-49620-89-G-0016DEF
9. PERFORMING ORGANIZATION NAME AND ADDRESS: Materials Research Laboratory, Tuskegee University, Tuskegee, AL 36088	10. PROGRAM ELEMENT, PROJECT, TASK AREA & WORK UNIT NUMBERS: 61102F, 2303/BS
11. CONTROLLING OFFICE NAME AND ADDRESS: AIR FORCE, OFFICE OF SCIENTIFIC RESEARCH, BOLLING AIR FORCE BASE, D.C. 20332-6448 NA	12. REPORT DATE: January 1991
	13. NUMBER OF PAGES: 42
14. MONITORING AGENCY NAME & ADDRESS (if different from Controlling Office): Summary #11	15. SECURITY CLASS. (of this report): Unclassified
	15a. DECLASSIFICATION/DOWNGRADING SCHEDULE

16. DISTRIBUTION STATEMENT (of this Report)

Approved for public release; distribution unlimited

17. DISTRIBUTION STATEMENT (of the abstract entered in Block 20, if different from Report)

18. SUPPLEMENTARY NOTES

19. KEY WORDS (Continue on reverse side if necessary and identify by block number)

Composites, Ceramics, Silicon Carbide / Silicon Carbide, High Temperature Flexure, Fracture.

20. ABSTRACT (Continue on reverse side if necessary and identify by block number)

This report describes the progress made during the second year of a two-year program funded by the United States Airforce, Office of Scientific Research, to develop experimental and analytical capability to characterize Ceramic/Ceramic composites at room and elevated temperatures.

DD FORM 1 JAN 73 1473 EDITION OF 1 NOV 65 IS OBSOLETE S/N 0102-LF-014-6601

Unclassified

SECURITY CLASSIFICATION OF THIS PAGE (When Data Entered)

ABSTRACT

The fracture and flexural behavior of monolithic SiC and SiC–whisker reinforced SiC composites (SiC_w/SiC) have been investigated at room and elevated temperatures. Flexure and fracture tests were conducted in a four–point beam configuration at 23^0C, 800^0C and 1200^0C to study the effects of whisker reinforcements especially in respect of mechanical and thermal stability at high energy environments. Flexural strengths and fracture toughness data within the test temperature range are presented in graphical as well as in weibull form, and experimental observations are analyzed and discussed. Attempts have been made to predict the flexural properties of the composite by coupling the principle of minimization of potential energy and the rule of mixture. The deflection curve of a composite four–point beam coupon is found from an assumed Fourier series solution satisfying the geometric boundary conditions and using the rule of mixture. Strain compatibility conditions are applied to determine the axial displacement field and hence the flexural strain. Stresses on the matrix and fiber are then estimated under the assumption of isostrain conditions.

TABLE OF CONTENTS

LIST OF FIGURES

LIST OF TABLES

1.0 INTRODUCTION

Ceramic matrix composites (CMC) have emerged in recent years as potentially excellent engineering materials because of their superior mechanical properties such as specific strength and stiffness at elevated temperature. These attractive thermo–mechanical properties of CMC's accompanied by their low moisture susceptibility and long term thermal stability at high energy environments have generated considerable interests among researches. Significant improvement have been observed in this decade in the manufacture of these composites. However, the very brittle nature of ceramics imparts one of their most undesirable properties – fracture toughness. Recent studies have shown that fracture toughness of monolithic ceramics can be moderately improved via the incorporation of whiskers into ceramic matrices [1–4]. Although the failure of the ceramic is still catastrophic, the whisker reinforcements has generated considerable interests because of its relatively simple manufacturing process, namely, the powder metallurgy method. Among various ceramic matrices, SiC is considered to be the most suitable for high temperature applications because of its mechanical integrity and resistance to oxidation and corrosion at elevated temperature. Due to this thermo–mechanical stability SiC are being extensively experimented as oxidation protection coating for Carbon/Carbon composites in aerospace applications [5,6].

Knowledge of the critical intensity factor, K_{Ic}, along with the elastic modulus, the defect size and the relative geometries of the defect and the structure make it possible to predict the failure stress of that structure. The fracture toughness approach, therefore, constitutes a useful failure criterion for ceramics [3]. With brittle matrices such as ceramics,

catastrophic failures are common once the fracture stress has been reached. Therefore, measure of fracture toughness of the composite is essentially a measure of success of its fabrication process and its use in structural applications. It has also been observed that the surface chemistry of whiskers in whisker–reinforced composites, plays a major role in forming the interface which in turn significantly controls the fracture toughness of the composites. It has been found that at elevated temperatures, presence of oxygen in some fibers triggers oxidation and the subsequent degradation of fibers causes considerable concern for high temperature applications. In the current research, whisker toughening of SiC matrix with SiC whiskers was considered to investigate the effects of temperature in the flexural strength and fracture toughness. Monolithic SiC was also tested at corresponding temperatures to study, and compare the improvements in the mechanical properties.

Both flexural strength and fracture toughness in this research were determined using four–point bend test. The governing equation [7–9] to compute the flexural stress in the beam is derived from the Bernoulli–Euler elastic beam theory based on the consideration of equilibrium alone. This does not provide us with a continuous displacement field that is often required for design purposes. Most importantly, the equation dose not consider anisotropy that exists in the beam materials due to its composite structure. In the current investigation, an attempt has been made to formulate a method based on the minimization of potential energy, and the rule of mixture to determine the displacement, flexural strain and flexural stress of a four–point beam.

2.0 EXPERIMENTAL WORK

2.1 Processing and Specimen Preparation:

The processing and hot pressing of monolithic SiC and SiC_w/SiC composite was carried out at the facilities of Cercom. The raw materials used were SiC powder supplied by Cercom, and SiC whiskers manufactured by Tokai Carbon. SiC whiskers used in this study were TWS–100. The manufacture's data for SiC whiskers and SiC powder are shown in tables 1 and 2.

SiC billet was supplied as "PAD" SiC, type B (Billet # 2–638–2f). The billet had fine grained micro structure, characteristic of pressure assisted densified "PAD" SiC. The hot pressing was carried out in an inert atmosphere at 2080 ^{0}C and 2500 psi pressure. The bulk density of the billet (Alpha SiC) was 3.18 g/cc and the average grain size was 1.9 – 2.2 microns.

The hot pressing of the composite billet was carried out in an inert atmosphere at 1750 ^{0}C and 3500 psi pressure. Hot pressing temperature was limited to 1750 ^{0}C as per recommendation of the manufacturer of SiC whiskers. A block diagram of the hot pressing technique is shown in Fig.1. The density of the composite billet was 3.225 g/cc. Billets of both monolithic SiC and SiC_w/SiC composites were prepared to study the improvements in flexural strength and fracture toughness values of the composite. All the specimen for the above tests were cut and machined at Bomas Machine Specialties. It was observed that whiskers tended to align in a direction perpendicular to the hot pressing direction.

pressing operation. Accordingly, proper care was taken during specimen machining so that the whisker orientation was perpendicular to the direction of applied load.

2.2 Measurement of Flexural Strength:

The flexural strength was measured for both monolithic SiC and Si_wC/SiC composites by using 4–point bend test. Instron 8502 test system with data acquisition system was used for conducting the tests. The 4–Point bend fixture was fabricated from cast SiC and the pull rods were made out of Alumina. The outer and inner spans of the fixture were 30 mm and 15 mm, respectively. The size of the test specimen used was 3 mm wide, 4 mm deep and 48 mm long, and is shown in Fig. 2. The cross head speed for all tests was 0.508 mm/minute (0.02 inches/minute). The equation used for evaluating flexural strength (4–point loading) is as follows [7].

$$S_{fl} = 3P\ (L-a)/2bd^2$$

where,

P = Applied load

L = Outer span

a = Inner span

b = width of the specimen

d = depth of the specimen

2.3 Measurement of Fracture Toughness:

Fracture toughness tests were carried out on Chevron notched specimens. The four

point bend fixture as mentioned earlier was used. The size of the specimen was same as that of the flexure specimen. The width of the Chevron notch was 0.2 mm as shown in Fig. 3. All tests were conducted at a cross head speed of 0.508 mm/minute (0.02 inches/minute). The equation used for evaluating the fracture toughness of chevron notched specimen by 4 point bend test is as follows [10,11]:

$$K_{1c} = \frac{P}{BW^{1/2}} Y \tag{1}$$

where,

$$Y = (2.92 + 4.52a_0 + 16.14\alpha_0^2).\frac{S_1 - S_2}{W}.\left(\frac{\alpha_1-\alpha_0}{1-\alpha_0}\right)^{0.5} \tag{2}$$

$$\alpha_0 = \frac{a_0}{W} \tag{3}$$

$$\alpha_1 = \frac{a_1}{W} \tag{4}$$

P = Applied load

W = Depth of the specimen

B = Width of the specimen

S_1= Outer span for loading the bar specimen

S_2= Inner span for loading the 4 point bar specimen

a_0= Initial notch length (distance from crack mouth to chevron vertex)

a_1= Distance from crack mouth to intersection of chevron notch & specimen edge

a = Crack length

3.0 PREDICTION BY ENERGY APPROACH

The technique of minimizing a particular energy expression and obtaining an approximate solution to the governing differential equation of elasticity is well established and are available in the literatures [12–14]. One of the more important of these techniques is the Rayleigh–Ritz method. In this method the total potential energy, Π is determined by summing up the total strain energy and the total work done, which in turn is estimated from an assumed displacement solution. The assumed displacement solution must satisfy the geometric boundary conditions, and contains unknown constants that are determined by minimizing Π with respect to each of the constants. The rule of mixture is introduced in this formulation with the assumption that both matrix and fiber will contribute to the composite stiffness, E_c in direct proportion to their own stiffness (E_m and E_f) and volume fractions (v_m and v_f). Once the deflection curve is determined, strain compatibility conditions are applied to find the axial displacement field using the symmetry boundary conditions. This yields axial strain which is assumed to be same for both matrix and fiber. Rule of mixture is then applied to compute the stress in the matrix, fiber and in the composite.

3.1 Deflection Solution

A typical four–point beam specimen is shown in Fig.2. The deflection of the beam is assumed to be a continuous function of x alone and approximate it by the following Fourier series. Let u and v be the axial and vertical displacements of the beam, respectively. We assume

$$v(x) = \sum_{n=1}^{\infty} a_n \, \text{Sin} \, \frac{n\pi x}{L} \tag{5}$$

such that $v(0) = v(L) = 0$ at the two supports of the beam, i.e. at $x = 0$ and $x = L$, respectively. Two simple supports at the two ends can not support any moment and we observe that

$$v''(x) = -\sum_{n=1}^{\infty} a_n \frac{n^2\pi^2}{L^2} \text{Sin} \, \frac{n\pi x}{L} \tag{6}$$

satisfies these two boundary conditions. Therefore four geometric boundary conditions, namely, deflection and moment, at each end of the beam are satisfied.

Let σ_x, σ_y, σ_z, τ_{xy}, τ_{yz}, and τ_{zx} be the state of stress that satisfies the stress equations of equilibrium, and is caused by the application of forces on the surface of the beam. If we denote U to be the total strain energy for the above mentioned stress state, we can then write [15]

$$U = \frac{1}{2} \int_v (\sigma_x \epsilon_x + \sigma_y \epsilon_y + \sigma_z \epsilon_z + \tau_{xy}\gamma_{xy} + \tau_{yz}\gamma_{yz} + \tau_{zx}\gamma_{zx}) dv \tag{7}$$

However, over the inner span, the beam is under pure bending and we can write $\sigma_x = \sigma$ and $\sigma_y = \sigma_z = \tau_{xy} = \tau = _{yz} = \tau_{zx} = 0$. Here σ denotes the bending or flexural stress on the beam due to the applied load. Therefore,

$$U = \frac{1}{2} \int_v \frac{\sigma^2}{E} dv \tag{8}$$

Under the pure bending $\sigma = \frac{My}{I}$ where M and I are respectively the applied moment and

the second moment of the cross–sectional area. The substitution reduces equation (8) to

$$U = \frac{1}{2}\int_0^L \frac{M^2}{EI}dx \tag{9}$$

It is to be noted here that $\sigma = \frac{My}{I}$ is based on the assumption of homogeneous material and the isotropic hooke's law. Therefore, eqn. (9) will be modified later by the rule of mixture. In terms of displacement v(x), we can write equation (9) as

$$U = \frac{1}{2}\int_0^L EI(\frac{d^2v}{dx^2})^2\,dx \tag{10}$$

where we have substituted $M = EI\frac{d^2v}{dx^2}$.

We know that E is not a constant over the volume and herein we introduce the rule of mixture to account for the multi phase materials of the beam specimen. Since the cross–sectional area of the specimen is constant along x, the distribution of E over x is taken from the simple rule of mixture such that

$$E_c = E_m v_m + E_f v_f \tag{11}$$

Where E_m, E_f, v_m, and v_f's are respectively the elastic modulii and volume fractions of the matrix and the fiber. Here we have assumed that $v_m + v_f = 1$, and both matrix and fiber contribute to the composite stiffness in direct proportion to their respective stiffnesses and volume fractions. Equation (10) therefore, takes the form

$$U = \frac{E_m v_m I}{2}\int_0^L EI\,(\frac{d^2v}{dx^2})^2\,dx + \frac{E_f v_f I}{2}\int_0^L EI(\frac{d^2v}{dx^2})^2 dx \tag{12}$$

We now proceed to determine the work done, W, on the beam by the applied loads.

We can write

$$W = \frac{P}{2}(v)_{x=\frac{L}{4}} + \frac{P}{2}\cdot(v)_{x=\frac{3L}{4}} \tag{13}$$

$$= \frac{P}{2}\left[\sum_{n=1}^{\infty} a_n \mathrm{Sin}\frac{n\pi}{4} + \sum_{n=1}^{\infty} a_n \mathrm{Sin}\frac{3n\pi}{4}\right] \tag{14}$$

We know from symmetric loading that $(v)_{x=\frac{L}{4}} = (v)_{x=\frac{3L}{4}}$

To conform to this condition, we restrict the values of n = 1, 3, 9, 11....etc. in the infinite series such that

$$W = P\sum_{n=1,3,9,11}^{\infty} a_n \mathrm{Sin}\frac{n\pi}{4} \tag{15}$$

The total potential energy, Π can therefore, be written as

$$\Pi = U - W = \frac{E_m v_m I}{2}\int_0^L EI\left(\frac{d^2v}{dx^2}\right)^2 dx + \frac{E_f v_f I}{2}\int_0^L EI\left(\frac{d^2v}{dx^2}\right)^2 dx - P\sum_{n=1,3,9,11}^{\infty} a_n \mathrm{Sin}\frac{n\pi}{4}$$

$$= \frac{I(E_m v_m + E_f v_f)}{2}\int_0^L \left[\sum_{n=1,3,9,11}^{\infty} a_n \left(\frac{n\pi}{L}\right)^2 \mathrm{Sin}\frac{n\pi x}{L}\right]^2 dx - P\sum_{n=1,3,9,11}^{\infty} a_n \mathrm{Sin}\frac{n\pi}{4} \tag{16}$$

Squaring the series and observing that

$$\int_0^L \mathrm{Sin}\frac{m\pi x}{L}\mathrm{Sin}\frac{n\pi x}{L}dx = 0, \text{ for } m \neq n$$

$$\text{and } \int_0^L \mathrm{Sin}\frac{m\pi x}{L}\mathrm{Sin}\frac{n\pi x}{L}dx = L/2, \text{ for } m = n,$$

we get

$$\Pi = \frac{\pi^4 I(E_m v_m + E_f v_f)}{4L^3} \sum_{n=1,3,9,11}^{\infty} a_n^2 n^4 - P \sum_{n=1,3,9,11}^{\infty} a_n \mathrm{Sin}\frac{n\pi}{4} \tag{17}$$

Now we apply the minimizing condition

$$\frac{\partial \Pi}{\partial a_m} = 0 \tag{18}$$

where all coefficients except a_m are taken as constant during the partial differentiation. Differentiating equations (17) according to equation (18) we find that

$$\frac{\pi^4 m^4 I(E_m V_m + E_f V_f)}{2L^3} \cdot a_m = P \, \mathrm{Sin} \, \frac{m\pi}{4}$$

$$\text{i.e,} \qquad a_m = \frac{\sqrt{2} \, PL^3}{\pi^4 m^4 I(E_m v_m + E_f v_f)} \tag{19}$$

for m = 1, 3, 9, 11 etc.

Therefore, the deflection of the composite beam can be found from equation (5) as

$$v(x) = \frac{\sqrt{2} \, PL^3}{\pi^4 I(E_m v_m + E_f v_f)} \sum_{n=1,3,9,11}^{\infty} \frac{1}{n^4} \mathrm{Sin}\frac{n\pi x}{L} \tag{20}$$

This expression will be used to compute the maximum deflection in the beam which will be compared with the experimentally found values.

3.2 Strain and Stress Solution

We have observed before that the existing stress in the beam is only $\sigma_x=\sigma$ with σ_y, σ_z, τ_{xy}, τ_{yz}, and τ_{zx} being zero. Under this condition, we can write the strain compatibility condition as

$$\frac{\partial v}{\partial x}+\frac{\partial u}{\partial y}=0 \tag{21}$$

From eqn. (21), with the help of eqn.(20), we can write

$$\frac{\partial u}{\partial y}=-\frac{\sqrt{2}\ PL^2}{\pi^3 I(E_m v_m+E_f v_f)}\sum_{n=1,3,9,11}^{\infty}\frac{1}{n^3}\mathrm{Cos}\frac{n\pi x}{L} \tag{22}$$

Integrating equation (22) with respect to y

$$u=-\frac{\sqrt{2}\ PL^2 y}{\pi^3 I(E_m v_m+E_f v_f)}\sum_{n=1,3,9,11}^{\infty}\frac{1}{n^3}\mathrm{Cos}\frac{n\pi x}{L}+f(x) \tag{23}$$

To find f(x), we apply the symmetry boundary condition, that at $x = L/2$, $u = 0$ for all values of y. This gives, $f(x) = 0$, therefore, we write

$$u=-\frac{\sqrt{2}\ PL^2 y}{\pi^3 I(E_m v_m+E_f v_f)}\sum_{n=1,3,9,11}^{\infty}\frac{1}{n^3}\mathrm{Cos}\frac{n\pi x}{L} \tag{24}$$

This is the general expression for u and we observe that it is a function of both x and y. From equation (24) we find the flexural strain, ϵ_x as

$$\epsilon_x = \frac{\partial u}{\partial x} = \frac{\sqrt{2}\ PLy}{\pi^2 I(E_m v_m + E_f v_f)} \sum_{n=1,3,9,11} \frac{1}{n^2} \mathrm{Sin} \frac{n\pi x}{L} \tag{25}$$

We will compute maximum strain in the composite beam according to equation (25) and compare with the experimental value. Assuming isostrain both in the matrix and fiber in the axial direction, we can write

$$\sigma_f = E_f \epsilon_x \text{ and } \sigma_m = E_m \epsilon_x \tag{26}$$

Where σ_m and σ_f are the stresses in the matrix and fiber. Using the rule of mixture we now find the flexural stress in the composite, σ_{comp} [16,17], as

$$\sigma_{comp} = \sigma_f V_f + \sigma_m (1 - V_f) \tag{27}$$

4.0 RESULTS AND DISCUSSION

4.1 Flexure and Fracture Tests:

Both monolithic SiC and SiC_w/SiC composites were tested at room and elevated temperatures for flexural strength and fracture toughness. Maximum deflection (v_{max}), maximum flexural strain and flexural strengths, obtained from the flexure test of SiC_w/SiC at various temperatures are shown in Table–3 through Table–5. The tables also show the average values of the test results for each category. Weibull analyses of flexural strength data for various temperatures are shown in Fig. 4. Fracture toughness tests were performed at 23^0C and 800^0C only. Tests at 1200^0C are in progress. Values of K_{ic} at two temperatures are shown in tabular form in Table–6. Corresponding weibull analysis is shown in Fig. 5. For monolithic SiC, corresponding data have been generated and are presented in similar form in Table–7 through table–9. A comparison of the flexural strengths of SiC_w/SiC with monolithic SiC, and the variation of strength with temperature is shown in Fig. 6. Weibull analysis of flexural strength for SiC is shown in Fig. 7. Fracture toughness values of SiC and the weibull analysis of K_{1C} are shown, respectively, in Table–10 and Fig. 8. The variation of elastic modulii of SiC_w/SiC composite and SiC with temperatures are shown in tables 11 and 12.

It is observed from the flexural stress data that the strength of SiC_w/SiC composite at room temperature increased approximately by 23% from that of the monolithic SiC. The improvement in strength is clearly due to the whisker reinforcement. However, Fig. 5. shows that this improvement does not continue throughout the range of the test temperatures. Beyond 900^0C, SiC_w/SiC appears to show lesser strength than that of SiC. The figure also reveals that the monolithic SiC remains stable up to 800^0C and then looses strength rapidly.

On the other hand, SiC_w/SiC composite looses strength more or less uniformly throughout the test temperature range, and at 1200^{0}C the strength values was found to be less than that of SiC. However, the decrease in flexural strength was gradual at elevated temperatures and there was no drastic loss in strength, suggesting a moderately stable system to sustain temporary overheating without any catastrophic failure [18.]. It is believed that the uncoated SiC whiskers underwent partial degradation at elevated temperature which led to early failures. SEM analyses scheduled to be performed later, will reveal more details in this aspect. From the fracture toughness data it is observed that the value of K_{1c} for SiC_w/SiC has increased from 3.43 to 5.96 by whisker reinforcement. This improvement in fracture toughness becomes more prominent at 800^{0}C. SiC_w/SiC composite maintains K_{1c} value at 5.83, whereas, for monolithic SiC, the value drops to 3.01. The improvement in K_{1c} both at room and elevated temperatures is obviously attributed to the fiber bridging and crack deflection due to the presence of whiskers. It is interesting to note from the maximum deflection and flexural strain data that the absolute values of both deflection and strain are smaller at elevated temperatures than those at room temperature. It is shown earlier that flexural stress has reduced at higher temperatures. From this contradictory manifestation of the experimental data it is difficult to visualize the cause of the failure of the specimen at elevated temperatures at a lesser strain value. Fracture toughness data show that both SiC_w/Sic and SiC have become more brittle (reduction in K_{1c} value) at higher temperatures. We believe this increase in brittleness is the cause of undergoing lesser strain at the failure condition. We also observe that in case of SiC_w/SiC composite, the reduction in fracture toughness value between 23^{0}C and 800^{0}C is 2.18%, and the corresponding reduction in flexural strain is 6.8%. In case of monolithic SiC, the reduction in K_{1c} value and the flexural strain value are, respectively, 12.24% and 26.65%. Therefore, it is observed that the reduction in failure strain is proportional to the reduction in the fracture toughness at elevated temperature.

It is observed from the weibull analysis of SiC_w/SiC at various temperatures that the weibull distribution, β lie between 17.275 and 28.81. These weibull distributions are the slope of the straight lines, and are shown in Figs. 4. and 5. as shape factors (SF). These values of β suggest a moderate scatter of flexural data at room and elevated temperatures. The corresponding weibull analyses for the monolithic SiC show close similarity except that the characteristic lives are different. These characteristic life values which are indicative of 63.2% percentile of the distribution, are independent of the weibull modulus, and are found to be less than but close to the tabulated average values. In case of fracture toughness analyses, however, different situations are observed between the composite and the monolithic SiC, especially in respect of β values. For SiC_w/SiC, the weibull distribution is seen to be very low compared to that of SiC. Besides high scatter in the fracture data, this low weibull distribution indicates more random behavior of SiC_w/SiC to chevron notch sensitivity both at room and elevated temperatures.

4.2 Energy Approach:

Values of Maximum deflection, flexural strain and flexural stress obtained from the four–point bend test as shown in the previous section at room temperature, have been considered in the energy approach as the basis of a comparison. Values for both monolithic SiC and SiC_w/SiC were compared. Using eqn. (10) for the monolithic material, and performing the similar derivations we can easily formulate

$$v(x) = \frac{\sqrt{2}PL^3}{\pi^4 E_m I} \sum_{n=1,3,9,11}^{\infty} \frac{1}{n^4} \mathrm{Sin}\frac{n\pi x}{L}, \tag{28}$$

$$\text{and } \epsilon_x = \frac{\sqrt{2}PLy}{\pi^2 E_m I} \sum_{n=1,3,9,11}^{\infty} \frac{1}{n^2} \mathrm{Sin}\frac{n\pi x}{L},$$

where E_m is the elastic modulus of monolithic SiC.

From eqn. (20) it is observed that the maximum deflection takes place at $x = L/2$. The series contains $1/n^4$ term which is highly convergent and, therefore, taking only two terms, i.e., with $n = 1$ and 3

$$v_{max} = \frac{\sqrt{2}\ PL^3}{\pi^4 I(E_m v_m + E_f v_f)}\left[1 - \frac{1}{81}\right]. \tag{29}$$

According to eqn. (25), we can compute maximum strain at $x = L/2$ and observing that it occurs at $y = d/2$, where d is the depth of the specimen. Eqn. (25), with two terms in the series, reduces to

$$(\epsilon_x)_{max} = \frac{\sqrt{2}\ PLd}{2\pi^2 I(E_m v_m + E_f v_f)}[1 - \frac{1}{9}]. \qquad (30)$$

Now taking this maximum strain under consideration, we can determine the flexural stress using eqns.(26) and (27). Computations have been carried out for both monolithic SiC and SiC_w/SiC using the following properties:

$E_m = 480.0 \times 10^9$ N/m^2, $E_f = 450.0 \times 10^9$ N/m^2,

$v_m = 0.7$, $v_f = 0.3$,

$I = bd^3/12 = 16 \times 10^{-12}$ m^4,

L = 0.03 m, and d = 0.004 m.

The comparison with the experimentally determined values are shown in Table–13 and Table–14.

5.0 CLOSURE

From the results of the investigation the following conclusions may be drawn

1. Reinforcement of SiC with SiC whiskers increases the flexural strengths of the composite at room temperature, and up to 800^0C. However, no improvement in strength is observed at 1200^0C.
2. It has been observed that SiC_w/SiC composite looses strength uniformly throughout the test temperature range, while the strength of the monolithic SiC does very rapidly only after 800^0C. This indicates a trend for SiC more towards catastrophic failure beyond 800^0C.
3. At elevated temperatures slight reduction in fracture toughness values of SiC_w/SiC composite is found, but a higher reduction is observed in case of monolithic SiC. The observed fracture behavior suggests that micro structural modification incorporated via whisker reinforcements, imparted resistance to crack growth both at room and elevated temperatures. This calls for a detailed analyses of the crack–tip damage process through SEM for a clearer understanding of the failure mechanisms in ceramics as well as in the composite.
4. The SiC_w/SiC composite as well as the monolithic SiC show similarity in weibull distribution both at room and elevated temperatures in respect of flexural strengths. However, in case of fracture toughness, there is a wide reduction in weibull shape factor with SiC_w/SiC composite.
5. A formulation based on Rayleigh–Ritz method is presented to compute the deflection of a composite four–point beam specimen that has been used in the current investigation for mechanical characterization. Axial displacement and strain equations are derived from the strain compatibility condition, and stress equations are established on the basis of the rule of mixture and the assumption of isostrain condition. Good correlation between the experimental and predicted values are observed in case of composite, while those for monolithic SiC are slightly off.

6.0 Acknowledgements

This work was supported by the United States Navy, office of naval research under grant no. N0014–86–K–0765, and by the United States Air Force, office of scientific research under grant no. F–49620–20–89–C–0016–DEF. The authors acknowledge this support with appreciation.

7.0 REFERENCES

1. Shang, J. K., Yu. W. and Ritchie, R. O., "Role of Silicon Carbide Particles in Fatigue Crack Growth in SiC–particulate–reinforced Aluminum Alloy Composites," Material Science and Engineering, V 102, 181–192 (1988).

2. Green, D. J., "Assurance of Structural Reliability in Ceramics," Proceedings of the International Symposium on Advances in Processing of Ceramics and Metal Matrix Composites," Halifax, August 20–24, 1989.

3. Huq. N. and Jeelani, S., "Fracture Toughness measurements on SiC/Al_2O_3 Composites," Journal of Material Science, Accepted for Publication.

4. Jeelani S., Saleekin, S. and Huq, A., "Effects of Reinforcement Geometry on the Mechanical Properties of SiC_w/Al_2O_3 Composites," Journal of Materials Science (Prepared for Publication).

5. Stein, B., Maahs, H. and Brewer, W., "Airframe Materials for Hypersonic Vehicles," Proceedings of NASA/DOD Conference, Cocoa Beach, FL, Jan. 22–23, 1986, pp. 1–23.

6. The Department of Defense, University Research Initiative Program announcement, February 1991.

7. Whitney, J. M., Daniel, I. M. and Pipes, B., Experimental Mechanics of Fiber Reinforced Composite Materials, Society for Experimental Stress Analysis, Monograph No. 4.

8. Instron Series IX Automated Materials Testing System Reference Manual, M–12–2–152 (a), pp. b–1 to b–6.

9. Zweben, C., Smith W. S. and Wardle, M. W., "Test Methods for Fiber Tensile Strength, Composite Flexure Modulus, and Properties of Fabric–Reinforced Laminates," Composite Materials: Testing and Design (Fifth Conference), ASTM STP 674, 1979, pp. 228–262.

10. Munz, D., Busbey, R. T. and Shannon, J. L., "Fracture Toughness Determination of Alumina Using Four–Point Bend Specimens With Straight–Through and Chevron Notches," Journal of the American Ceramic Society, Vol. 63, No. 5–6 (1980).

11. Munz, D. J., Shannon, J. L. and Busbey, R. T., "Fracture Toughness Calculation from Maximum Load in Four–Point Bend Tests of Chevron Notch Specimens," International Journal of Fracture, 16R, 137–141 (1980).

12. Chou, P. and Pagano, N., Elasticity, D. Van Nostrand Company, Inc., Princeton, New Jersey, 1967.

13. Segerlind, L., Applied Finite Element Analysis, 2nd. Edition, John Wiley and Sons, New York, 1984.

14. Budynas, R., Advanced Strength and Applied Stress Analysis, McGraw–Hill Book Company, New York, 1975.

15. Jones, R. M., Mechanics of Composite Materials, Hemisphere Publishing Corporation, New York, 1975.

16. Yong, B. K. and Kim, C. H., "The Effect of Whisker Length on the Mechanical Properties of Alumina–SiC Whisker Composites," Journal of Material Science, 24 (1989), 1589–1593.

17. Fukuda, H. and Chow, W.., "A Probabilistic Theory of the Strength of Short–Fiber Composites With Variable Fiber Length and Orientation," Journal of Materials Science 17 (1982), 1003–1011.

18. Lamicq, P. J., Bernhart, G. A. Dauchier, M. M. and Mace, J. G., "SiC/SiC Composite Ceramics," American Ceramic Society Bulletin, 65 [2], 336–338, (1986).

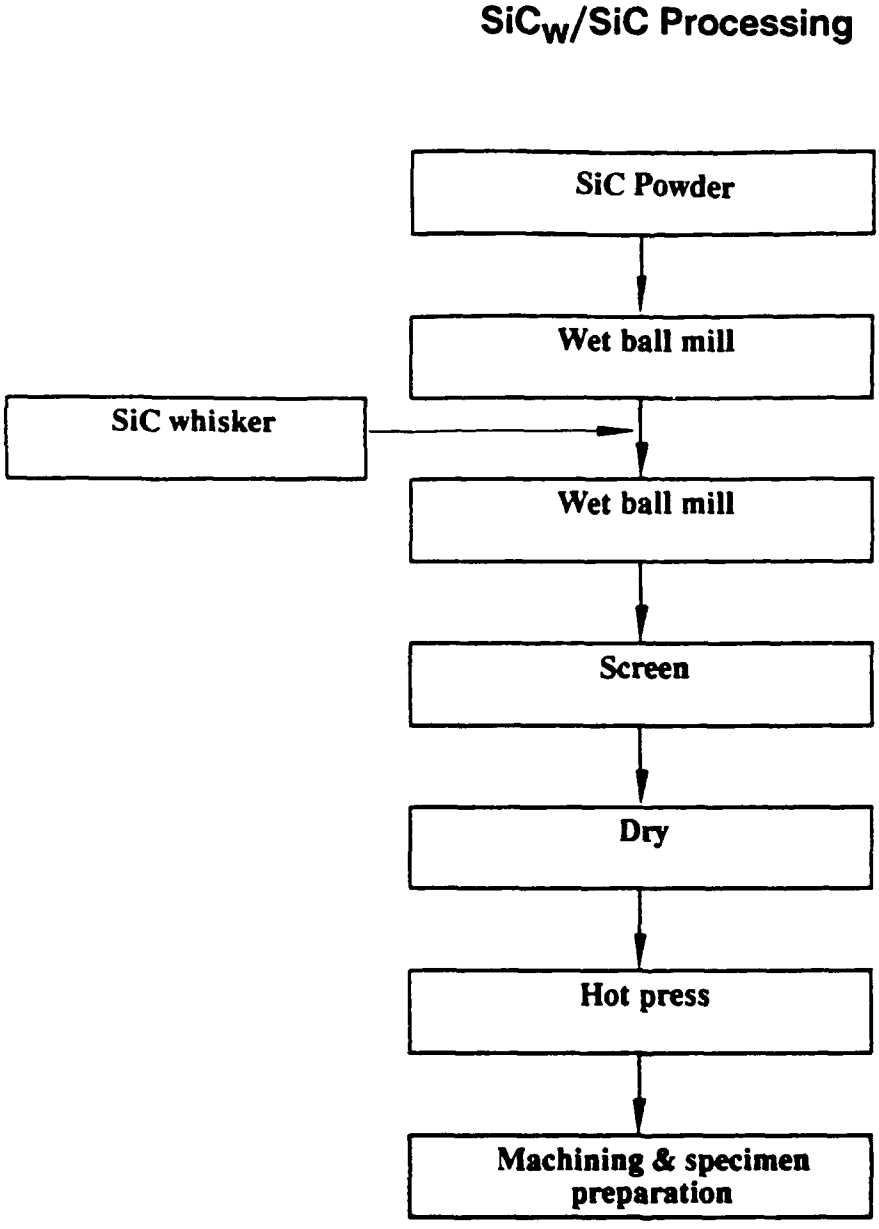

Figure 1. Block Diagram of the Processing of SiC_w/SiC Composites

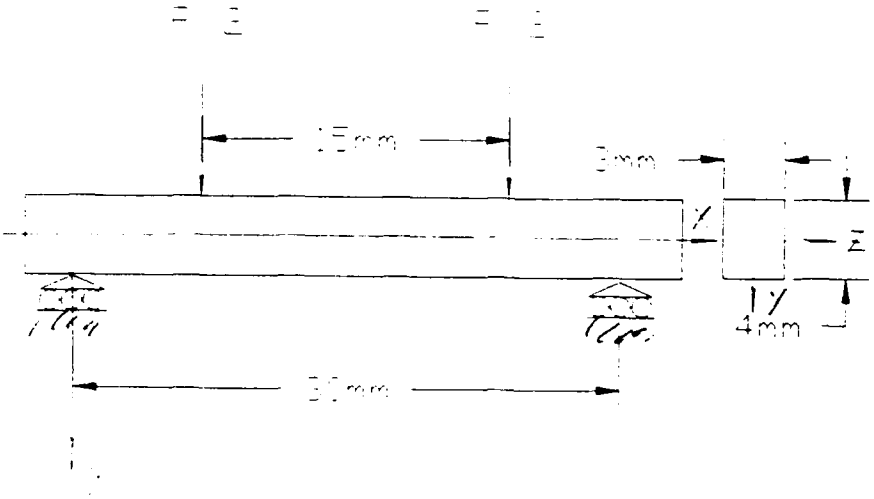

Figure 2. Four–Point Beam Specimen

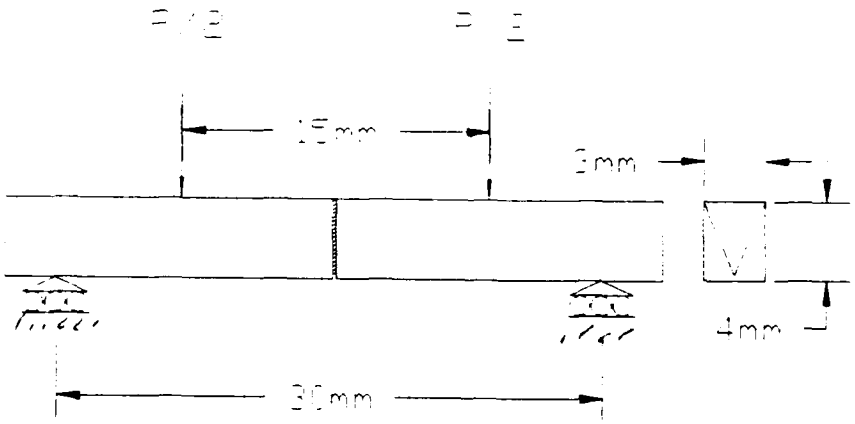

Figure 3. Chevron Notched Specimen

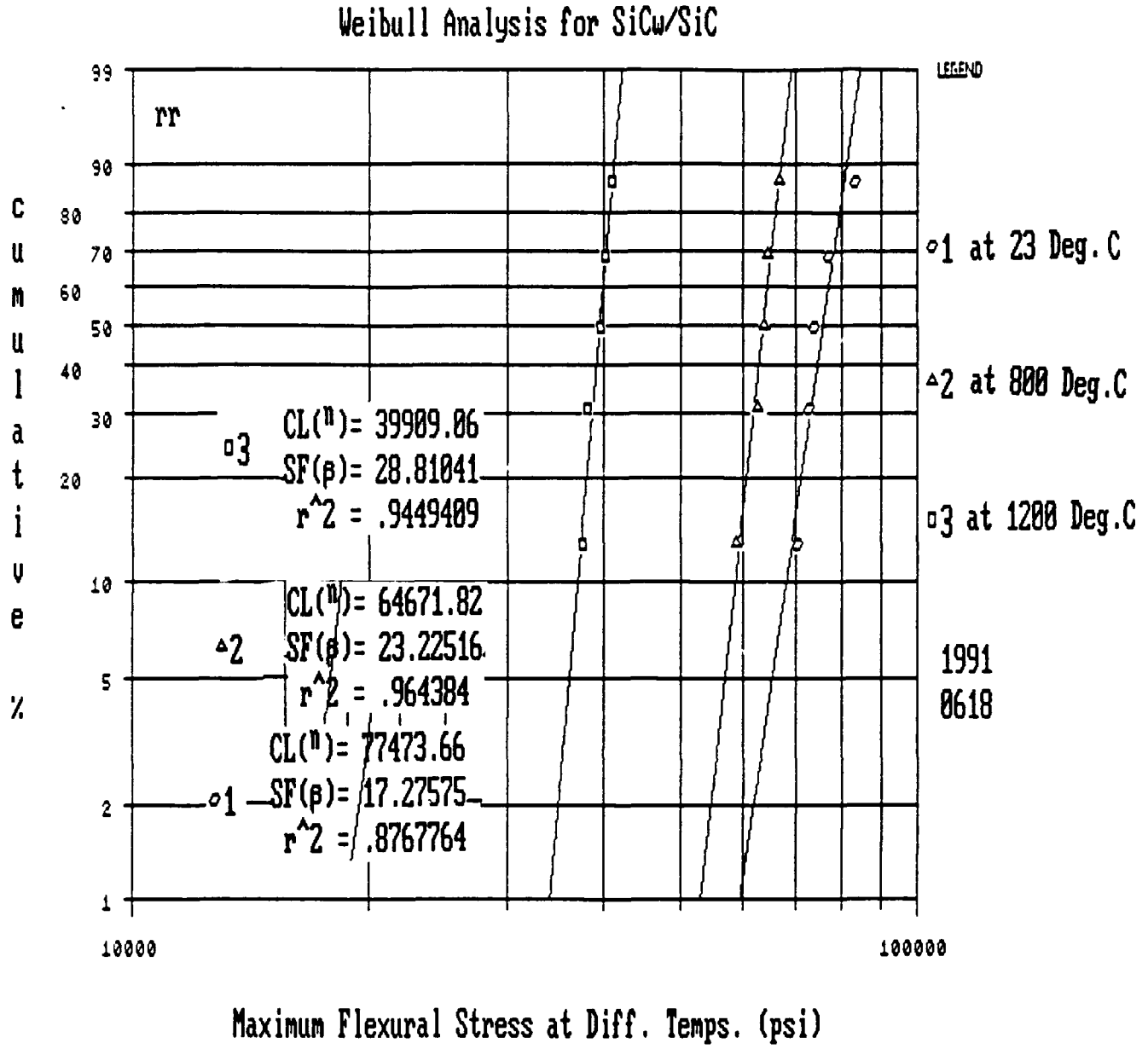

Figure 4. Weibull Analysis for Flexural Strength of SiC_w/SiC Composites.

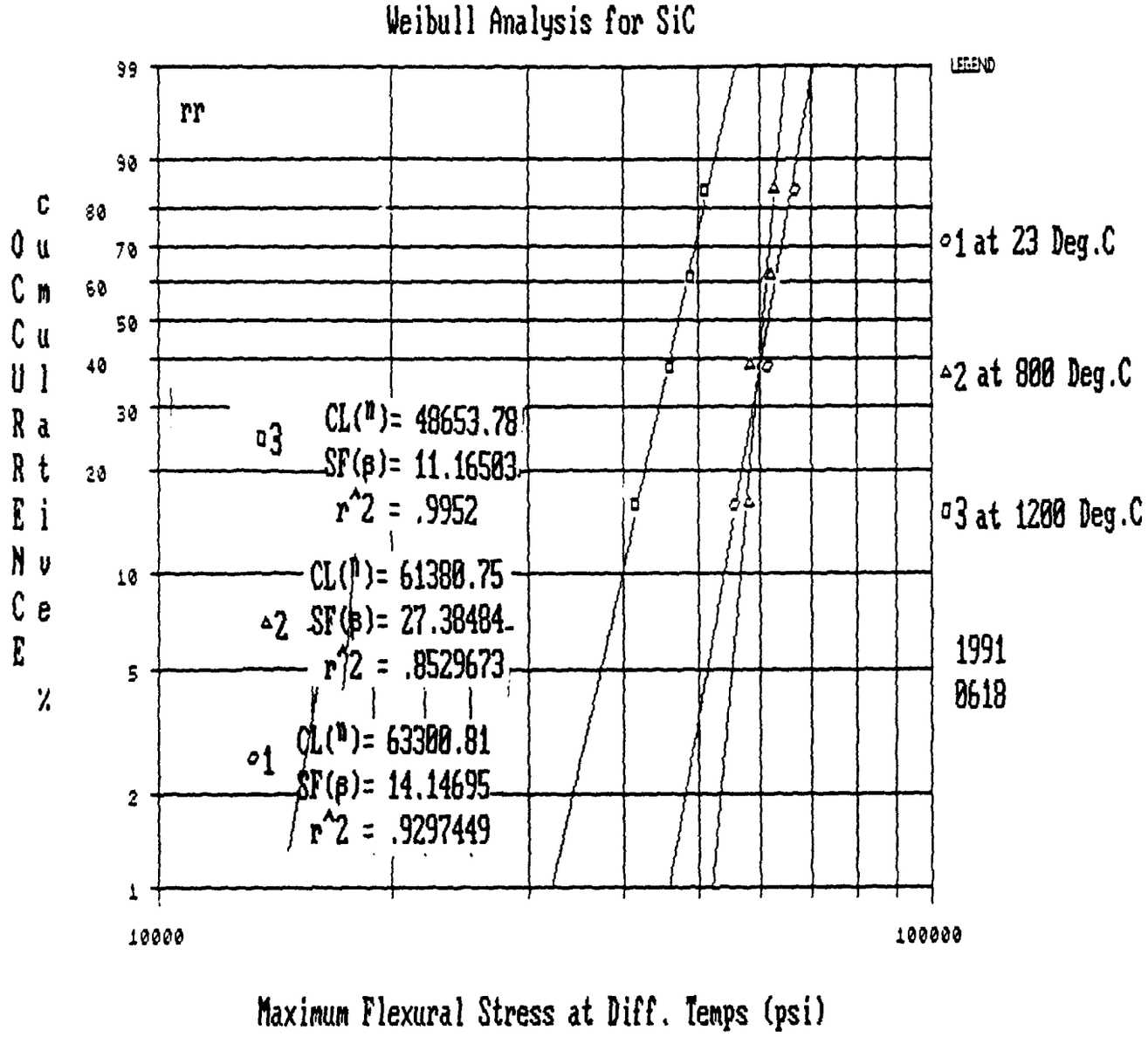

Figure 5. Weibull Analysis for Flexural Strength of SiC.

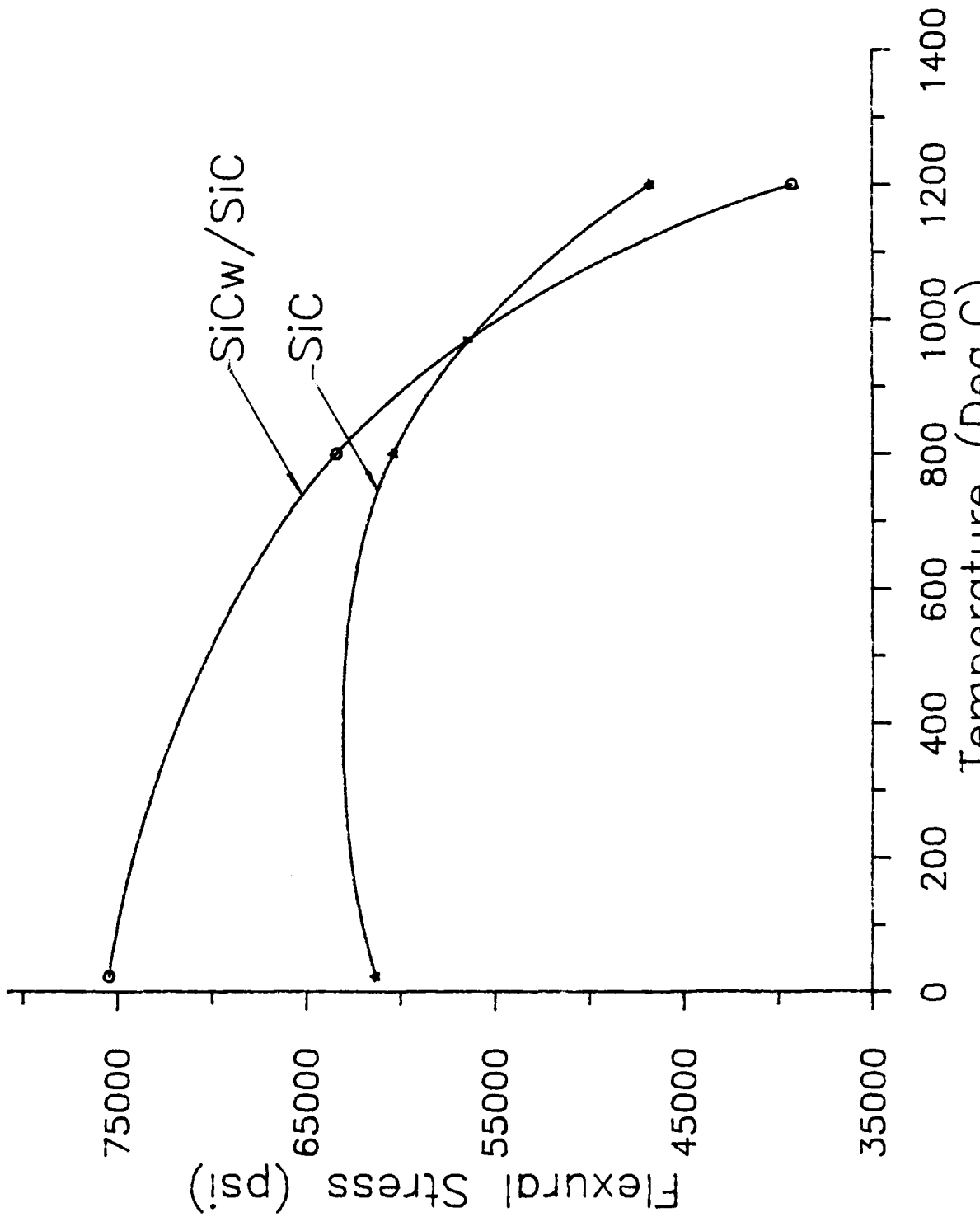

Figure 6. Flexural Strength Variation With Temperatures.

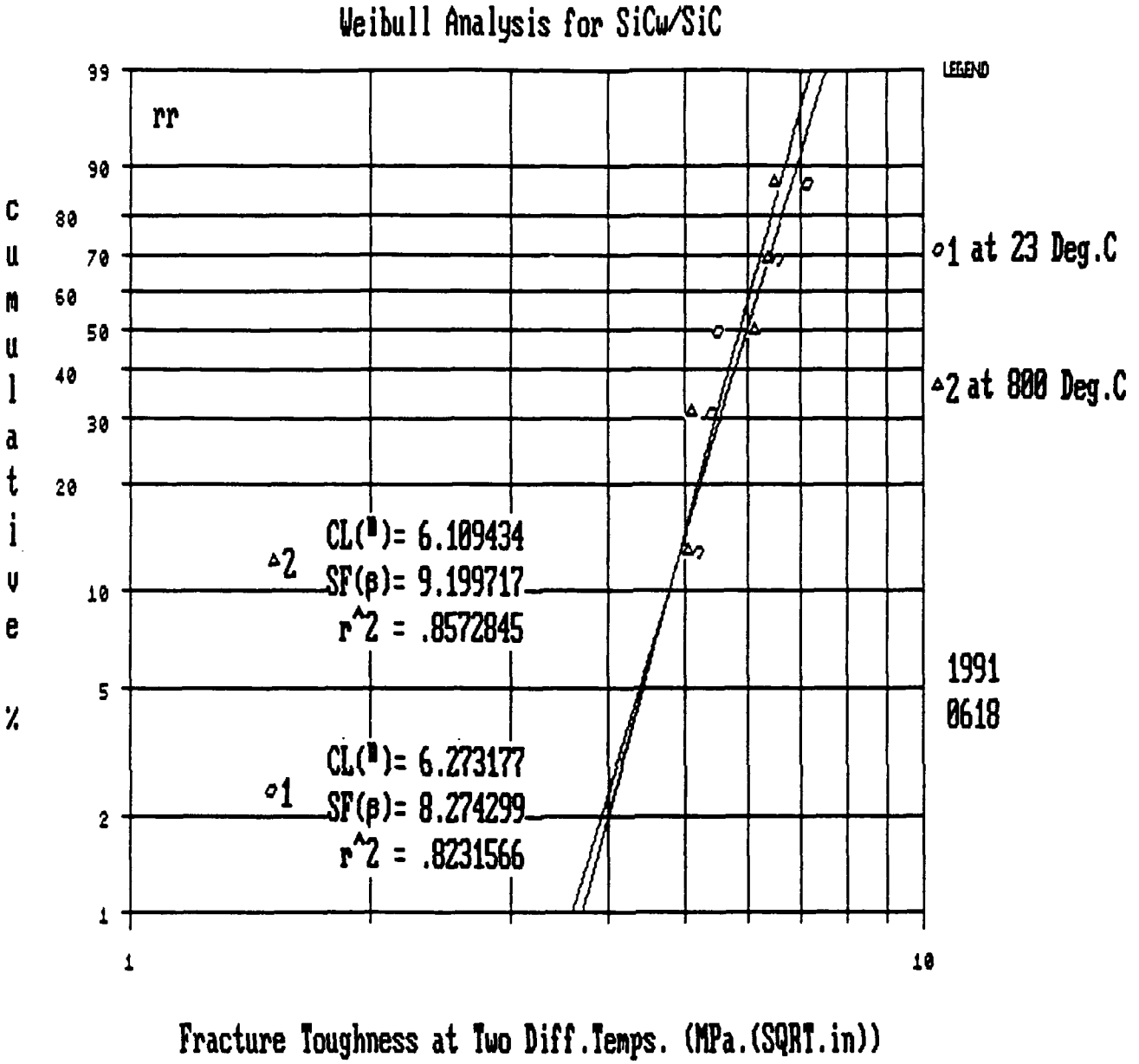

Figure 7. Weibull Analysis for Fracture Toughness of SiC_w/SiC Composites.

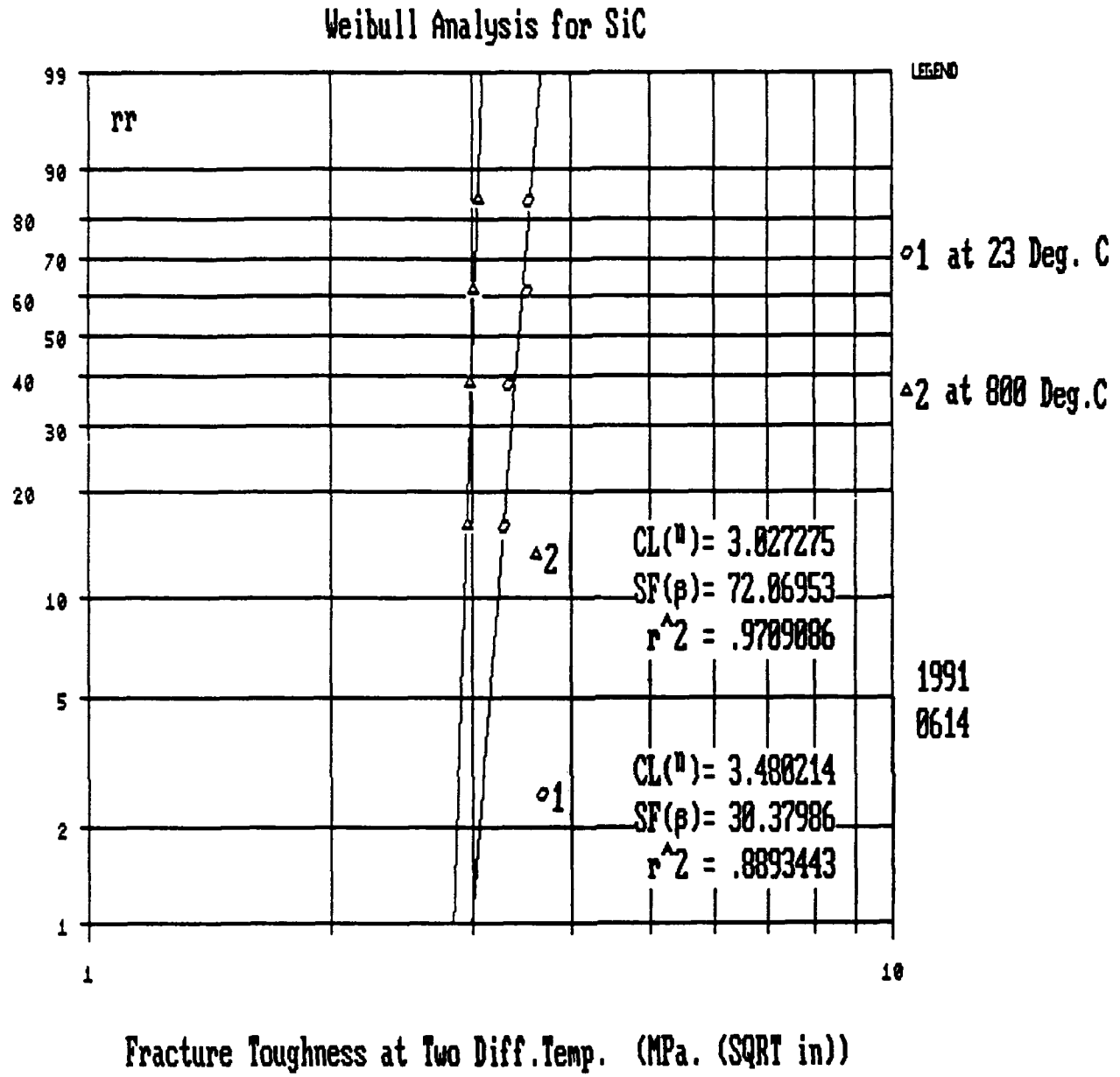

Figure 8. Weibull Analysis for Fracture Toughness of SiC.

Table 1: Manufacturer's data for the Physical properties of Silicon Carbide whiskers.

SiC Whisker: TWS-100	
1. Diameter	0.3 - 0.6 microns
2. Length	5.0 - 15.0 microns
3. Density	3.20 g/cc
4. SiC (Weight %)	99
5. SiO2 (Weight %)	< 0.5
6. Particulate Content	< 1.0 %
7. Crystal Type	Beta
8. Aspect Ratio	10 - 40
9. S.S.A	2-4 m^2/g

Manufacturer: Tokai Carbon Company.

TABLE 2: Manufacturer's Data for SiC Powder.

Silicon Carbide Powder: Cercom SiC, Type B	
1. Iron	0.05 %
2. Calcium	< 0.04 %
3. Aluminum	1.46 %
4. Titanium	0.028 %
5. Nitrogen	0.5 %
6. Total Oxygen Content	1.06 %
7. Free Carbon	0.74 %
8. Average Particle Size	1.0 microns
9. Density	3.216 g/cc
10. Specific Surface Area	6.1 sq.m/g

Serial Number	Maximum Deflection at 23°C, V_{max} (in)	Maximum Deflection at 800°C, V_{max} (in)	Maximum Deflection at 1200C, V_{max} (in)
1	0.002095	0.001555	0.00145
2	0.00184	0.001685	0.00147
3	0.00254	0.001718	0.00152
4	0.00257	0.001565	0.001505
5	0.00172	0.002065	0.00147
Average	**0.002153**	**0.001717**	**0.001483**

TABLE: 3 - Maximum Flexural Deflection for SiC_w/SiC

Serial Number	Maximum Flexural Strain at 23°C, (in/in)	Maximum Flexural Strain at 800°C, (in/in)	Maximum Flexural Strain at 1200°C, (in/in)
1	0.00103	0.000767	0.000715
2	0.00091	0.000831	0.000725
3	0.001253	0.000847	0.000749
4	0.001267	0.000772	0.000742
5	0.000848	0.001018	0.000725
Average	**0.001062**	**0.0008470**	**0.000731**

TABLE: 4 - Maximum Flexural Strain for SiC_w/SiC

Serial Number	Maximum Flexural Stress at 23°C, (lb/in^2)	Maximum Flexural Stress at 800°C, (lb/in^2)	Maximum Flexural Stress at 1200°C, (lb/in^2)
1	67,730	62,847	40,990
2	72,010	64,554	37,500
3	72,800	63,914	38,110
4	80,250	58,915	40,150
5	70,450	66,627	39,530
Average	**72,648**	**63,371.4**	**39,256**

TABLE: 5 - Maximum Flexural Stress for SiC_w/SiC

Serial Number	Fracture Toughness at 23^0C, K_{ic} ($MPa.in^{1/2}$)	Fracture Toughness at 800^0C, K_{ic} ($MPa.in^{1/2}$)
1	5.19	6.37
2	7.15	6.49
3	5.50	5.11
4	6.54	6.11
5	5.41	5.05
Average	5.96	5.83

TABLE: 6 - Fracture Toughness for SiC_w/SiC

Serial Number	Maximum Flexural Deflection at 23°C, V_{max} (in)	Maximum Flexural Deflection at 800°C, V_{max} (in)	Maximum Flexural Deflection at 1200°C, V_{max} (in)
1	0.002345	0.00132	0.00124
2	0.00305	0.001572	0.00104
3	0.00225	0.00140	0.00121
Average	**0.002548**	**0.001431**	**0.001163**

Table: 7 - Maximum Flexural Deflection for SiC

Serial Number	Maximum Flexural Strain at 23°C, V_{max} (in/in)	Maximum Flexural Strain at 800°C, V_{max} (in/in)	Maximum Flexural Strain at 1200°C, V_{max} (in/in)
1	0.001157	0.000651	0.00060
2	0.00150	0.000775	0.00051
3	0.00111	0.000690	0.00060
Average	0.001256	0.0007053	0.000573

TABLE: 8 - Maximum Flexural Strain for SiC

Serial Number	Maximum Flexural Stress at 23°C, V_{max} ($lb/in^{1/2}$)	Maximum Flexural Stress at 800°C, V_{max} ($lb/in^{1/2}$)	Maximum Flexural Stress at 1200°C, V_{max} ($lb/in^{1/2}$)
1	64,260	58,489	48,800
2	66,000	62,725	41,380
3	73400	58,062	50,990
Average	**67,887**	**59,758.6**	**47,056.6**

TABLE: 9 - Maximum Flexural Stress for SiC

Serial Number	Fracture Toughness at 23°C, K_{ic} ($MPa.in^{1/2}$)	Fracture Toughness at 800°C, K_{ic} ($MPa.in^{1/2}$)
1	3.30	3.06
2	3.54	2.96
3	3.35	2.99
4	3.52	3.02
Average	**3.43**	**3.01**

TABLE: 10 - Fracture Toughness for SiC

Serial Number	Modulus of Elasticity at 23°C, 10^6(psi)	Modulus of Elasticity at 800°C, 10^6(psi)	Modulus of Elasticity at 1200°C, 10^6(psi)
1	66.658	80.339	56.24
2	83.273	76.155	50.735
3	57.747	73.929	49.864
4	64.263	74.832	53.058
5	84.292	64.136	53.497
Average	**71.246**	**73.878**	**52.679**

TABLE: 11 - Modulus of Elasticity for SiC_w/SiC

Serial Number	Modulus of Elasticity at 23°C, 10^6(psi)	Modulus of Elasticity at 800°C, 10^6(psi)	Modulus of Elasticity at 1200°C, 10^6 (psi)
1	56.53	88.079	77.958
2	36.292	79.291	79.169
3	54.231	82.440	83.869
Average	49.0176	83.270	80.332

TABLE: 12 - Modulus of Elasticity for SiC

SPECIMEN No.	LOAD (lbs.)	DISPLACEMENT 10^{-3} (in)		FLAXURAL STRAIN 10^{-3} (in/in)		FLAXURAL STRESS 10^{4} (lbs/in^2)	
		ENERGY	EXPT.	ENERGY	EXPT.	ENERGY	EXPT.
1	218.8	1.93	2.345	0.968	1.157	6.7425	6.4260
2	182.7	1.613	3.05	0.809	1.50	5.6300	6.6000
3	201.4	1.778	2.25	0.89	1.11	6.2063	7.3400
MEAN	200.97	1.774	2.55	0.889	1.256	6.1929	6.7887

Table 14. **Comparison of Experimental and Energy Approach Data for SiC**

SPECIMEN No.	LOAD (lbs.)	DISPLACEMENT 10^{-3} (in)		FLAXURAL STRAIN 10^{-3} (in/in)		FLAXURAL STRESS 10^{4} (lbs/in^2)	
		ENERGY	EXPT.	ENERGY	EXPT.	ENERGY	EXPT.
1	225.5	2.03	2.095	1.017	1.03	6.9489	6.7730
2	252.9	2.275	1.84	1.14	0.91	7.7932	7.2010
3	242.1	2.178	2.54	1.092	1.253	7.4604	7.2800
4	272.6	2.452	2.57	1.23	1.267	8.4003	8.0250
5	239.3	2.153	1.72	1.0794	0.845	7.3741	7.0450
MEAN	246.48	2.2176	2.153	1.112	1.062	7.5954	7.2648

Table 13. Comparison of Experimental and Energy Approach Data for SiC_w/SiC